

# Comparison of hybrid FDG PET/MRI compared with PET/CT in colorectal cancer staging and restaging: a pilot study

Raj Mohan Paspulati,<sup>1</sup> Sasan Partovi,<sup>1</sup> Karin A. Herrmann,<sup>1</sup> Smitha Krishnamurthi,<sup>2</sup> Conor P. Delaney,<sup>3</sup> Nghi C. Nguyen<sup>4</sup>

<sup>1</sup>Department of Radiology, UH Case Medical Center, 11100 Euclid Ave, Cleveland, OH 44106, USA

<sup>2</sup>Department of Medicine-Hematology and Oncology, UH Case Medical Center, 11100 Euclid Ave, Cleveland, OH 44106, USA

<sup>3</sup>Department of Surgery-Colorectal, UH Case Medical Center, 11100 Euclid Ave, Cleveland, OH 44106, USA

<sup>4</sup>Radiology Department, UPMC Presbyterian, 200 Lothrop St, Pittsburgh 15213, PA, USA

## Abstract

**Purpose:** We report our initial clinical experience from a pilot study to compare the diagnostic accuracy of hybrid PET/MRI with PET/CT in colorectal cancer and discuss potential PET/MRI workflow solutions for colorectal cancer.

**Methods:** Patients underwent both FDG PET/CT and PET/MRI (Ingenuity TF PET/MRI, Philips Healthcare) for rectal cancer staging or colorectal cancer restaging. The PET acquisition of PET/MRI was similar to that of PET/CT whereas the MRI protocol was selected individually based on the patient's medical history. One nuclear medicine physician reviewed the PET/CT studies and one radiologist reviewed the PET/MRI studies independently. The diagnostic accuracy of each modality was determined in consensus, using available medical records as a reference.

**Results:** Of the 12 patients enrolled, two were for initial staging and ten for restaging. The median scan delay between the two modalities was 60 min. The initial imaging was PET/CT in nine patients and PET/MRI in three patients. When PET/CT was performed first, the SUV values of the 16 FDG avid lesions were greater at PET/MRI than at PET/CT. In contrast, when PET/MRI was performed first, the SUV values of the seven FDG avid lesions were greater at PET/CT than at PET/MRI. PET/MRI provided more detailed T staging than PET/CT. On a per-patient basis, with both patient groups combined for the evaluation of N and M staging/restaging, the true positive rate was 5/7 (71%) for PET/

CT and 6/7 (86%) for PET/MRI, and true negative rate was 5/5 (100%) for both modalities. On a per-lesion basis, PET/CT identified 26 of 29 (90%) tumor lesions that were correctly detected by PET/MRI. Our proposed workflow allows for comprehensive cancer staging including integrated local and whole-body assessment.

**Conclusions:** Our initial experience shows a high diagnostic accuracy of PET/MRI in T staging of rectal cancer compared with PET/CT. In addition, PET/MRI shows at least comparable accuracy in N and M staging as well as restaging to PET/CT. However, the small sample size limits the generalizability of the results. It is expected that PET/MRI would yield higher diagnostic accuracy than PET/CT considering the high soft tissue contrast provided by MRI compared with CT, but larger studies are necessary to fully assess the benefit of PET/MRI in colorectal cancer.

**Key words:** PET/MR—PET/CT—Rectal carcinoma—Liver metastases

The use of imaging in the staging and restaging of colorectal cancers has been evolving and improving in the last two decades. Magnetic resonance imaging (MRI) is an accepted modality for staging of rectal cancer, allowing an accurate identification of transmural invasion of the mesorectal fat and mesorectal fascia involvement [1, 2]. Computed tomography (CT) significantly lacks resolution of soft tissue contrast so that its utility in T staging of rectal cancer is limited. Due to the higher sensitivity and specificity compared with CT, FDG PET is recommended for use in a metastatic

workup for colorectal cancer [3]. Hybrid positron-emission tomography/computed tomography (PET/CT) imaging using F-18 fluorodeoxyglucose (FDG) has been shown to improve lesion localization and diagnostic confidence compared to FDG PET imaging alone [4].

In treatment monitoring and follow-up, CT is very valuable because of its ability to delineate tumor size and visceral involvement, and has been adopted to measure tumor response by Response Evaluation Criteria in Solid Tumors (RECIST) criteria [5, 6]. MRI has proven to be valuable to assess local therapy response [7] and to re-stage patients with colorectal cancer [8]. FDG PET appears to be better than CT and MRI in predicting response to preoperative therapy of locally advanced rectal cancer [9]. In a study comparing FDG PET/CT with whole-body MRI at 1.5 and 3 T in patients with recurrent colorectal cancer, PET/CT was found to be more accurate than MRI in lymph node metastases (sensitivity 93% vs. 63%). Both modalities were similarly appropriate for the detection of organ metastases (sensitivity 78% for PET and 80% for MRI) [10]. The overall diagnostic accuracy was 91% for PET/CT (sensitivity 86%, specificity 96%) and 83% for MRI (sensitivity 72%, specificity 93%) [10]. Nonetheless, FDG PET/CT had limited accuracy in the detection of small liver lesions, which were better depicted with MRI [8].

Recently, several hybrid PET/MRI systems have been introduced to clinical practice, which have addressed the technical challenges concerning the coregistration of PET and MRI data. Considering the aforementioned complementary advantages of PET and MRI, the use of a hybrid PET/MRI could serve as a one-stop imaging approach that potentially improves diagnostic confidence and accuracy in colorectal cancer. In this article, we report our initial clinical experience from an ongoing pilot study comparing the diagnostic accuracy of FDG PET/MRI with FDG PET/CT in rectal cancer staging and colorectal cancer restaging and discuss about workflow optimization for hybrid PET/MRI imaging dedicated for colorectal cancer.

## Materials and method

### *Patient population*

Twelve adult patients (three female and nine male; median age 59 years) were enrolled for this prospective study. Three patients had disease stage IIA, one patient IIIA, two patients IIIB, two patients IIIC, and four patients IVA. Two patients were scheduled for a clinical FDG PET/CT of the torso and MRI of the pelvis for rectal cancer staging because they were found to have high-risk or advanced rectal cancer—defined by T3 stage or higher, or known N1 stage or higher, or the presence of distant metastasis. Ten patients were referred for clinical FDG PET/CT for restaging of colorectal cancer, with or without the request of a diagnostic MRI. The

study was approved by the institutional review board (IRB), and all subjects signed a written consent form.

### *PET/CT scanning*

The PET/CT scanning of the torso was performed on a Gemini TF PET/CT scanner (Philips Healthcare). The glucose level was not measured prior to the FDG injection; however, all patients fasted at least 6 h prior to the FDG administration. A median dose of 470 MBq FDG (range 352–525 MBq) was administered, which was used for PET scanning at both PET/CT and subsequent PET/MRI. The PET data were acquired at 150 s/bed (range 90–180 s). The CT parameters were 120 kVp, 100 mAs (patient weight  $\leq 150$  pounds), or 150 mAs (patient weight  $> 150$  pounds) with slice thickness 5 mm. No oral or intravenous contrast was used. After completion of the PET/CT scanning of the torso, the patient underwent additional imaging of the pelvis after emptying the bladder. In 9 of 12 patients, the PET/CT was performed prior to PET/MRI, with an uptake of 61 min (range 57–74 min). The PET/CT scanners and PET/MRI scanner were located on the same floor of the building and approximately 60 m apart from each other.

### *PET/MRI scanning*

The PET/MRI examination was performed on a sequential PET/MRI scanner system (Ingenuity TF PET/MRI, Philips Healthcare) [11, 12]. The PET acquisition of the torso remained the same at PET/CT and PET/MRI. Unlike PET/CT, no additional PET imaging of the pelvis was obtained.

The PET/MRI examination was performed after PET/CT in 9 subjects at an FDG uptake of 136 min (range 120–159 min). In the other three patients, however, the PET/MRI was performed before PET/CT, which was aimed at testing and developing a PET/MRI workflow for colorectal cancer. They received the FDG administration while lying on the PET/MRI table and after some of the non-enhanced MR sequences had been completed. The remaining MR sequences ensued prior to PET scanning at an uptake of 60, 75, and 80 min. PET/CT was then performed at 94, 105, and 120 min after FDG injection, respectively.

At PET/MRI, a 3D multi-station spoiled gradient echo sequence, so called “atMR”, of the torso preceded the PET scanning to obtain attenuation correction of PET data, deriving from a 3-segment model accounting for air, lung, and soft tissue [12]. Although the diagnostic MR sequences were individually selected based on the patient’s medical history and prior imaging findings, the mDIXON images of the torso (3 mm slice thickness) are most valuable for the anatomical correlation with PET images [12]. For the abdomen, the standard MR sequences included T2-weighted TSE sequence, single shot

without fat saturation (5 mm slice thickness); axial diffusion-weighted imaging (DWI) with (apparent diffusion coefficient) ADC maps; pre- and post-gadolinium dynamic T1-weighted 3D THRIVE with fat suppression (1.5 mm slice thickness). For the pelvis, the standard sequences were high-resolution T2-weighted TSE (3 mm slice thickness) without fat saturation for rectal cancer staging; T2-weighted TSE, single shot without fat saturation (5 mm) for restaging; and axial DWI with ADC mapping [12, 13].

MRI contrast agents were used in 7 of 12 patients (dose range 10–20 mL). Three patients received rectal gel (60 mL) to aid the assessment of suspected rectal lesions as well as intramuscular glucagon (1 mg), which was administered while they were lying on the PET/MRI scanner, followed immediately by FDG injection. Subsequently, the MRI was acquired prior to PET with an uptake of 60 min and greater. The PET/MRI was acquired prior to PET/CT in these three patients receiving glucagon injection.

### Reference standards

Histopathology was available in eight of ten restaging patients to verify the nature of the lesions seen on PET/CT or PET/MRI. Only imaging follow-up was available in the two other patients. In patients referred for rectal cancer staging, histopathology of the primary lesions but not the pelvic lymph nodes was available. Otherwise, the nature of the lesions (malignancy vs. benign) was determined based on the consensus between the two readers with the consideration of available medical records.

### Image interpretation and data analysis

PET/CT and PET/MRI images were reviewed on a MIM workstation, version 6.1 (MIM Software<sup>TM</sup>, Cleveland, Ohio). One nuclear medicine physician reviewed the PET/CT studies and one radiologist reviewed the PET/MRI studies independently. The clinical indication for the scan was the only clinical information disclosed to

the readers. In a separate reading session, the two readers shared and discussed their findings and determined the diagnostic accuracy of each modality in consensus, using available histopathology as well as clinical and imaging follow-up as a reference.

Only equivocal or suspicious lesions for malignancy on either PET/CT or PET/MRI were considered for correlative measurements. A maximum of three lesions of each body area or organ (e.g., lung, mediastinum, liver, abdomen, and pelvis) were included in the measurements. The lesion size in axial diameter on either CT or MRI and maximum standard uptake value (SUVmax), defined as [tissue concentration (MBq/g) × body weight (g)]/[injected dose (MBq)] were obtained. In addition, physiologic radiotracer activity was measured in the liver and blood pool; a circular 1.5 cm region-of-interest (ROI) was placed in the co-registered PET/CT and PET/MRI images at the mid aspect of the right liver lobe as well as the proximal aspect of the aortic lumen to obtain the SUVmax within these ROIs. None of the ROI for the liver was placed in proximity of a liver metastasis. Besides SUVmax, we used also SUVmax ratio, defined as lesion SUVmax/ liver SUVmax to correlate the lesion uptake between PET/CT and PET/MRI.

### Statistical analysis

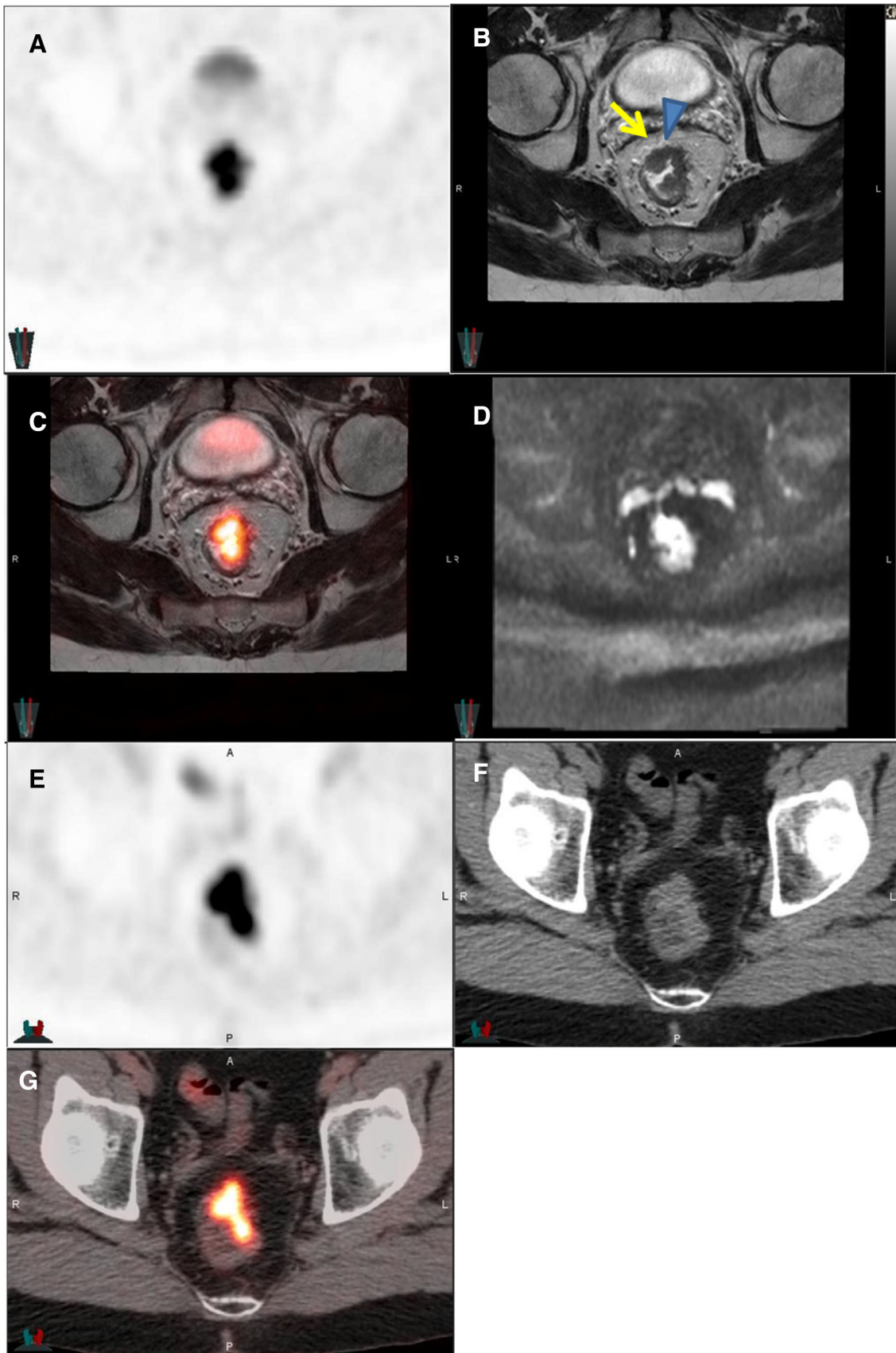
Patient characteristics were assessed using measures of central tendency (median, minimum–maximum) and frequencies (%) for categorical variables. Descriptive statistics (median, minimum–maximum) was used to summarize the SUV findings. No specific statistical test was performed due to the small sample size. The statistical software MedCalc, Version 12.7.1, was used.

## Results

The examination time was shorter at PET/CT including the additional pelvic imaging (median 38 min, range 25–47 min) compared with PET/MRI (median 97 min, range 65–137 min). The median delay between PET/CT

**Table 1.** SUV characteristics in physiologic regions (blood pool, liver) and FDG avid lesions in the nine patients, in which the PET/CT was performed prior to the PET/MRI

	PET/CT, SUVmax	PET/MR, SUVmax
Blood pool (9 patients, PET/CT first)	1.9 (1.2–2.52)	1.3 (0.8–1.6)
Liver (9 patients, PET/CT first)	2.3 (1.7–3.4)	2.1 (1.6–3.4)
	PET/CT, SUVmax	PET/MR, SUVmax
PET/CT first (16 lesions)	3.0 (0.5–25.5)	3.9 (1.6–21.6)
PET/MRI first (7 lesions)	5.9 (3.4–8.0)	4.3 (2.3–6.3)
	PET/CT, SUVmax ratio	PET/MR, SUVmax ratio
PET/CT first (16 lesions)	2.0 (0.2–11.1)	2.5 (0.8–10.8)
PET/MRI first (7 lesions)	2.7 (1.5–7.2)	2.0 (1.2–7.0)





◀**Fig. 1.** 58-year-old man with recently diagnosed moderately differentiated adenocarcinoma of the rectum was referred for staging with PET/CT and MRI. PET/MR images—axial PET (A), T2W TSE (B), fused PET/T2W TSE (C), DWI (D)—showed focal intense FDG uptake (SUVmax 25.5) of a rectal mass in the proximal rectum. T2W TSE image (B), shows transmural infiltration of the mesorectal fat (*arrow*) without involvement of the mesorectal fascia (*arrowhead*), consistent with a T3 stage. PET/CT images—axial PET (E), CT (F), and fused PET/CT (G)—show focal intense FDG uptake (SUVmax 21.6) fusing onto rectal wall thickening. However, it is not able to provide appropriate T staging because the muscularis propria and mesorectal fascia are not visible. Subcentimeter pelvic lymph nodes are not FDG avid at both modalities and thought to be benign. Subsequently, the patient underwent chemoradiation followed by surgical resection. PET/CT was acquired before PET/MR with a delay of 58 min. Mesorectal fascia (*triangle*).

and PET/MRI examinations was 60 min (range 30–95 min). PET/CT was performed first in the nine subjects, in which the SUVmax values of the blood pool were higher compared with those at PET/MRI, Table 1. When PET/CT was performed first, the SUVmax and SUVmax ratio of the 16 FDG avid lesions were greater at PET/MRI than at PET/CT. In contrast, when PET/MRI was performed first, the SUVmax and SUVmax ratio of the 7 FDG avid lesions were greater at PET/CT than at PET/MRI, Table 1. Among the three patients administered with glucagon, PET scanning was associated with markedly increased skeletal muscular uptake in one patient, which negatively affected the PET interpretation. In the other two patients, the skeletal muscular uptake was slightly elevated but did not affect the image interpretation. Among the nine patients without glucagon administration, the skeletal muscular uptake was normal in seven patients and slightly elevated in two patients, which however did not affect the image interpretation.

For the two patients with rectal staging, both imaging modalities showed no evidence of loco-regional lymph node metastasis or distant metastasis. Unlike PET/CT, however, PET/MRI provided detailed T staging showing a T3 rectal lesion in both patients as well as mesorectal fascia involvement in one patient (Fig. 1), which was supported by histopathology and endoscopic ultrasound. These patients underwent neoadjuvant chemoradiation followed by surgical resection. With staging and restaging patients combined, PET/MRI shows at least comparable accuracy in N and M staging/restaging to PET/CT. On a per-patient basis, the true positive rate was 5/7 (71%) for PET/CT and 6/7 (86%) for PET/MRI, and true negative rate was 5/5 (100%) for both modalities. The false negative rate of 14% (one of seven patients) for PET/MRI was attributed to the fact that it missed to diagnose liver metastases in one patient. The false negative rate of 29% (two of seven patients) was higher for

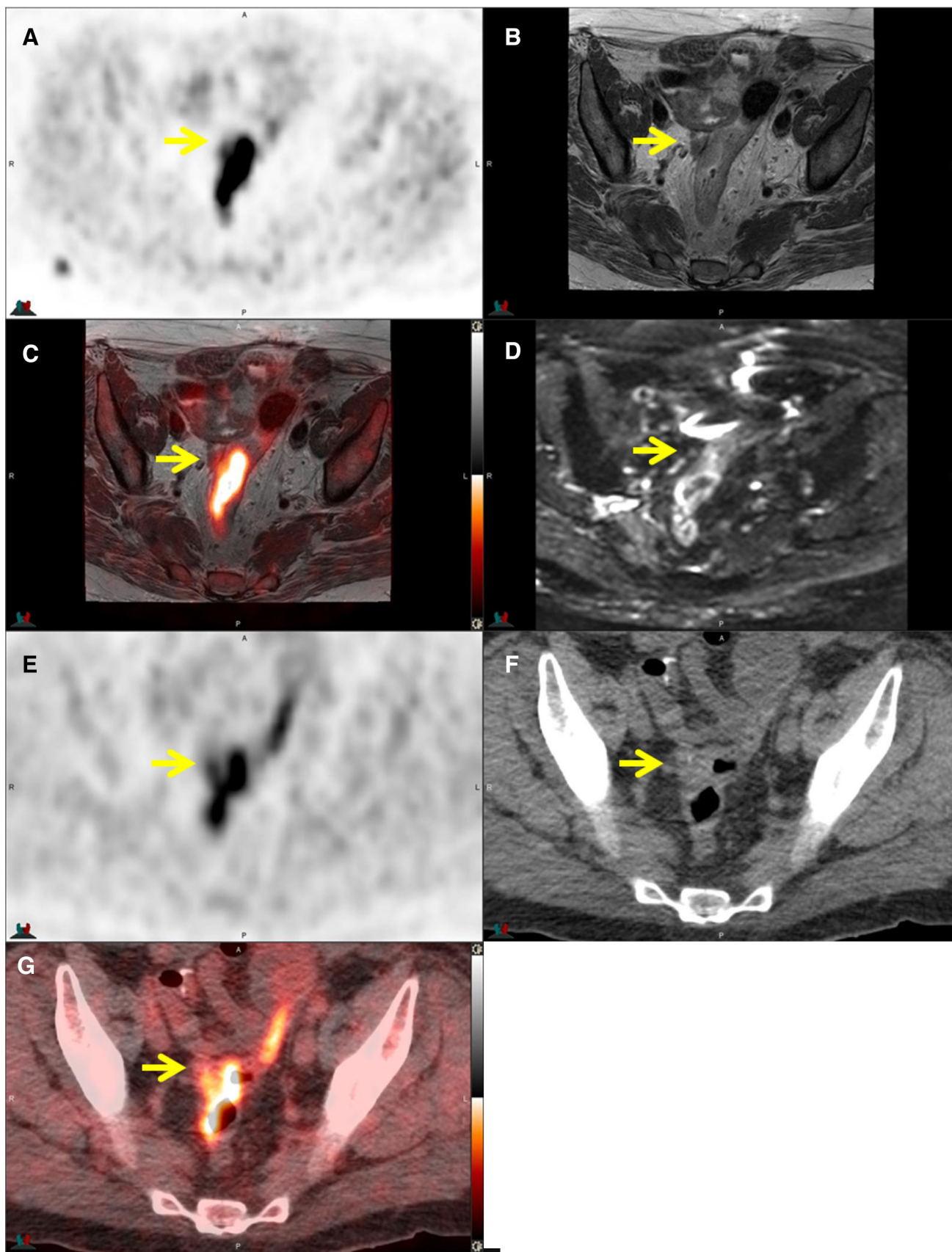
PET/CT because it failed to diagnosis rectal and perirectal metastatic implants in one additional patient, which was correctly identified by PET/MRI, Fig. 2. Both PET/CT and PET/MRI failed to identify early signs of liver metastases in one patient, in which the MR examination of the abdomen 3 months later showed several new contrast-enhanced liver lesions; subsequent core biopsy confirmed metastatic liver disease. In retrospect, there was one subcapsular 6 mm contrast-enhancing lesion in the right liver lobe on mDIXON images that did not show FDG avidity. The MRI protocol was however not optimized for liver imaging in this patient, lacking the high-resolution MR images.

On a per-lesion basis, PET/CT identified 26 of 29 lesions (90%) that were correctly detected by PET/MRI lesions (16 lymph nodes metastases, 13 distant metastases). PET/CT failed to identify three lesions compared with PET/MRI, which involved two rectal and perirectal metastatic implants in one patient (Fig. 2), and one additional  $0.7 \times 0.7$  cm<sup>2</sup> right paraspsoas node besides other abdominal lymphadenopathy, and liver metastases in another patient. In one patient, the CT images of the PET/CT showed evidence of bone erosion caused by a presacral soft tissue lesion. Although this lesion was detected at PET/MRI, the bone erosion was however not visible on the MR images, Fig. 3.

## Discussion

The recent introduction of hybrid PET/MRI offers new opportunities for cancer imaging and diagnosis. To our knowledge, this is the first report on the diagnostic performance of hybrid PET/MRI in colorectal cancer staging and restaging. Although with only 12 patients enrolled in this ongoing clinical trial, we have already gained valuable information about the strengths and weaknesses of PET/MRI compared with PET/CT as well as the workflow of PET/MRI in colorectal cancer that we would like to share with the readers. In the current study, PET/MRI shows its strengths in rectal cancer T staging. With staging and restaging patients combined, PET/MRI shows at least comparable accuracy in N and M staging as well as restaging to PET/CT.

In a recent publication, Drzezga et al. [14] and Wiesmueller et al. [15] reported on their first clinical experiences with integrated PET/MRI (Biograph mMR, Siemens) based on 32 and 46 oncologic patients, and showed that PET/MRI image quality and lesion detection were comparable with PET/CT. The patient population however was heterogeneous including a variety of malignancies ranging from malignant melanoma, breast cancer to colon cancer. Drzezga et al. [14] did include four cases of colon cancer and two cases of rectal cancer, and Wiesmueller et al. [15] included three cases of rectal cancer, but they did not evaluate for the diagnostic accuracy of PET/MRI and PET/CT. Our study was



◀**Fig. 2.** 58-year-old man with a history of pT4aN0Mx adenocarcinoma of the sigmoid colon referred for PET/CT 26 months after initial diagnosis. PET/MR images—axial PET (**A**), high-resolution T2W TSE (**B**), fused PET/T2W TSE (**C**), DWI (**D**)—show rectal wall thickening of 6 cm in length with associated FDG avidity (SUVmax 10.3) and an adjacent  $1.7 \times 1.1 \text{ cm}^2$  FDG avid right perirectal soft tissue density, suspicious for rectal and perirectal metastatic implant (*arrow*). PET/CT images—axial PET (**E**), CT (**F**) and fused PET/CT (**G**)—also show intense uptake (SUVmax 9.0) along the rectum; however, the increased rectal uptake was interpreted as physiologic uptake. In retrospect, there is a small focus of intense uptake adjacent to the rectum (*arrow*), corresponding to the metastatic implant detected at PET/MRI. Exploratory laparotomy 3 months later showed multiple rectal and perirectal metastatic implants. PET/CT was acquired before PET/MR with a delay of 38 min.

however designed to compare the diagnostic accuracy of these modalities in rectal cancer staging and colorectal cancer restaging. The current study demonstrates the high accuracy and important role of high-resolution MRI in determining the T stage of rectal cancer, as was the case in our two patients [1, 2]. Neither PET scanning at PET/MRI nor PET/CT scanning provides additional relevant information to T staging besides MRI. PET/MRI is expected to be more accurate than PET/CT in N and M staging as well considering the high soft tissue contrast provided by MRI compared with CT [8], but future research is warranted in this regard.

On a per-patient basis, the true positive rate was 5/7 (71%) for PET/CT and 6/7 (86%) for PET/MRI, and true negative rate was 5/5 (100%) for both modalities for N and M staging/restaging. The false negative rate of 14% for PET/MRI was attributed to the fact that it missed to diagnose liver metastases in one patient. It is well known that FDG PET may miss small liver metastases (<1 cm) because of the underlying physiologic uptake within the liver [16]. Although MRI has been proven reliable in diagnosing liver metastasis [8], small lesions, particularly those in the subcapsular region may be difficult to be diagnosed with high confidence. In addition, dedicated MR sequences of the liver (T2W, DWI, and dynamic contrast-enhanced T1W) were not obtained in this patient with a history of rectal cancer. The false negative rate of 29% (two of seven patients) was higher for PET/CT because it also missed to diagnosis rectal and perirectal metastatic implants in one additional patient, which was correctly identified by PET/MRI. Although there was intense FDG uptake along the rectum at both modalities, the CT was not helpful in delineating the rectal wall thickening as well as the mesenteric implants. In contrast, MR images provided great anatomical details, and in combination with PET, the diagnostic confidence of PET/MRI for identifying these metastases was high. In addition, given the fact that MRI with liver protocol is better than CT in detecting liver metastases,

the overall diagnostic accuracy for PET/MRI is expected to be higher than that of PET/CT [8, 17].

On a per-lesion basis, both modalities were concordant in 26 of 29 lesions (90%), which is no surprise because of the combination of anatomical and functional imaging at PET/MRI and PET/CT. However, PET/CT failed to identify three lesions compared with PET/MRI, which involved two rectal and perirectal metastatic implants in one patient, and one additional  $0.7 \times 0.7 \text{ cm}^2$  right paraspsoas node in another patient. Although PET/MRI detected the additional paraspsoas node compared to PET/CT, this may be because PET/CT was acquired first, which allowed the lesion to further accumulate metabolism until the PET/MRI was performed [18, 19]. MRI would have missed this small node had there been no focal FDG uptake on PET to guide for anatomical correlation. The potential weakness of PET/MRI is demonstrated in one patient, in which the CT images of PET/CT but not the MRI images of PET/MRI was able to identify bone erosion caused by a presacral lymph node [20]. An MRI protocol with dedicated bone marrow sequence would be required to improve the detection of bone cortex/marrow involvement. The early identification of bone erosion may have significant implication for clinical follow-up and patient management to prevent skeletal-related events [21].

The observed differences in SUV values within physiologic structures (liver, blood pool) are mainly attributed to radiotracer pharmacokinetics over time between PET/CT and PET/MRI scanning. Using the same scanner systems as in the current report, Kershah et al. has shown that the blood pool activity is lower at PET/MRI than PET/CT when PET/CT was acquired first [22]. On the other hand, the higher metabolism measured in tumor lesions at PET/MRI compared to PET/CT is related to the fact that the FDG uptake does not end at the standard duration of 60 min, but it could gradually increase over several hours [22, 23].

PET/MRI workflows for various oncological indications are currently being validated at our institution. The workflow for colorectal cancer will be the most challenging one because it requires not only standard PET/MRI scanning of the torso but also regional MRI scans dedicated to the liver and pelvis. A standard PET/MRI protocol would entail a 60-min uptake phase in a quiet room separate from the scanner system, followed by imaging, which could be either PET first or MRI first depending on the clinical situation. We adhered to this standard protocol in nine of the 12 patients. In three patients, however, we administered the radiotracer while the patient was lying on the PET/MRI scanner table, started with the MRI immediately afterward, and completed the PET portion at the end. This approach may be acceptable for PET imaging of the torso, but it is not recommended for the examination of the brain because the noise of MRI may affect the PET brain images later



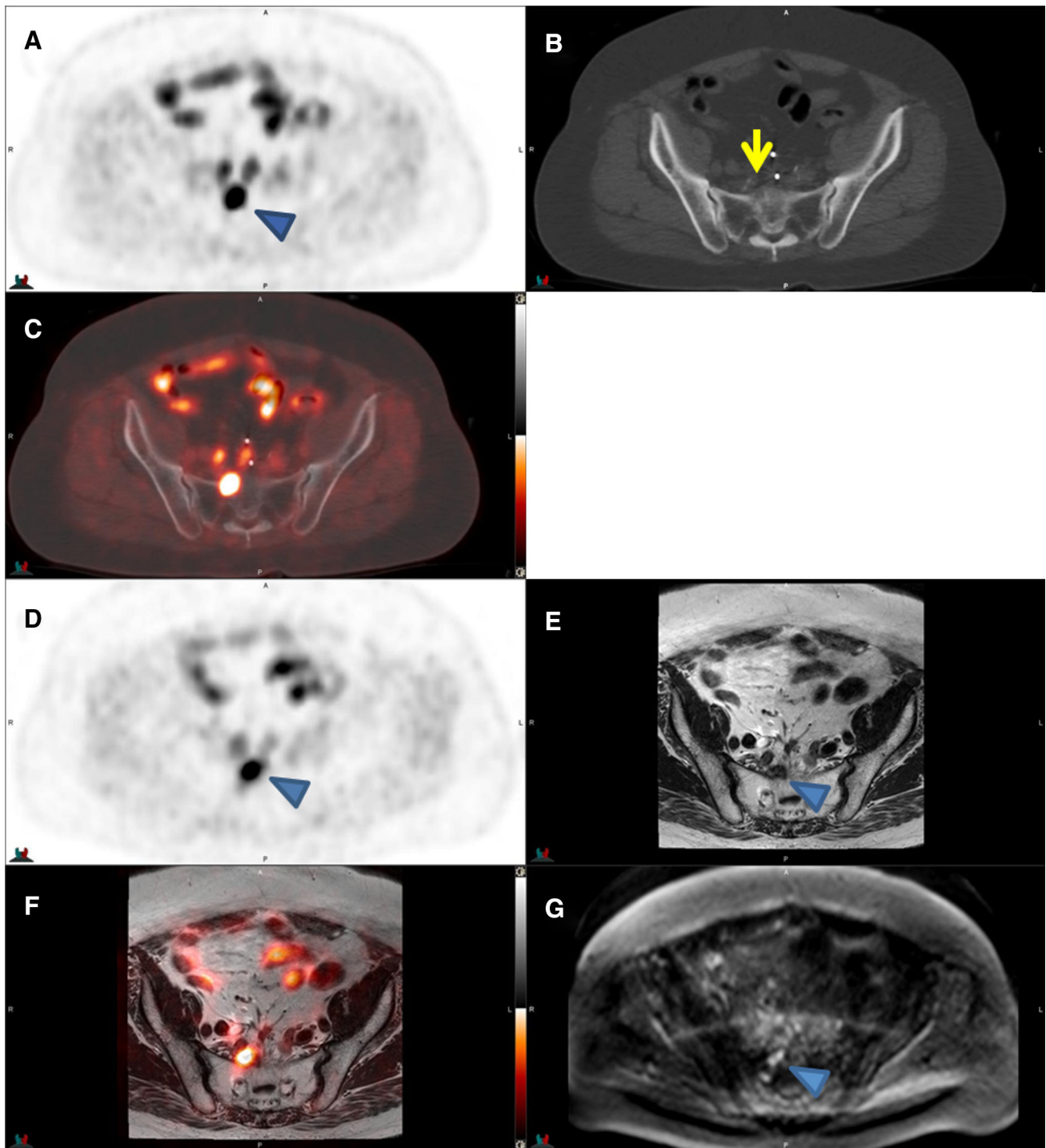


**Fig. 3.** 72-year-old man with a history of pT3N0M0 rectosigmoid colon carcinoma and rising CEA levels was referred for restaging with PET/CT 22 months after initial diagnosis. PET/CT images—axial PET (**A**), CT (**B**), fused PET/CT (**C**)—show a  $1.3 \times 1.0$  cm<sup>2</sup>, intensely FDG avid presacral lymph node (*arrowhead*, SUVmax 14.1) with evidence of erosion of S1 (*arrow*). PET/MR images—axial PET (**D**), T2W

TSE (**E**), fused PET/T2W TSE (**F**), and DWI (**G**)—demonstrate the FDG avid lesion (SUVmax 13.6) in the same region (*arrowhead*) but there is no visible erosion of S1. There are several larger FDG avid mesenteric lymph nodes in this region at both modalities, not shown. PET/CT was acquired before PET/MR with a delay of 64 min.

[24]. Another challenge involves the administration of glucagon prior to MRI acquisition to help reduce bowel motion and artifacts during MRI scanning. If adminis-

tered before the PET scanning, glucagon may affect the PET images because it causes a shift of FDG from the blood into the skeletal muscles [25], as was present in one



		FDG			Glucagon			
<b>A</b>	FDG uptake	atMR & mDIXON (H,N,C)	PET (H,N,C)	Bladder void	atMR & mDIXON (A,P)	PET (A,P)	Diagnostic, pre-Gd MRI (A,P)	Diagnostic, post-Gd MRI (A,P)
	60 min	5 min	10 min	10 min	5 min	10 min	15 min	15 min
		15 min			45 min			
	Total procedure: 130 min							

		FDG					
<b>B</b>	FDG uptake (60 min)	Diagnostic, pre-Gd MRI (A,P)	Diagnostic, post-Gd MRI (A,P)	Bladder void	atMR & mDIXON (N,C,A,P)	PET (N,C,A,P)	
		25 min	25 min	10 min	10 min	20 min	
		50 min			30 min		
	Total procedure: 90 min						

**Fig. 4.** Proposed workflow designs for colorectal cancer imaging with the Ingenuity TF PET/MRI. Workflow A—uptake phase before scanning. This workflow is applicable for scanning with and without glucagon administration. If clinically indicated, glucagon for the MRI is administered after completion of PET scanning and will not affect the PET images. Although it is time intensive for the patient (procedure time 130 min), the scanning time is shorter compared with workflow B (60 vs. 80 min). It also provides good patient comfort with acquisitions of 15 and 45 min each, and has the advantage that other MR sequences may be added if the patient tolerates the additional scanning. Workflow B—uptake

phase during MRI scanning. This workflow suits best for scanning without glucagon administration. A glucagon administration for MRI scanning will likely affect the PET images later. This workflow is time effective for the patient (procedure time 90 min) because the FDG uptake occurs while the patient is being scanned with MRI. It allows also plenty of time for the MRI examination of the abdomen and pelvis (50 min), taking into account the 60-min FDG uptake. Imaging of the head (H) is not recommended given the potential interference of MRI noise on the FDG PET images. *H* head, *N* neck, *C* chest, *A* abdomen, *P* pelvis.

of three patients in this report. If clinically indicated, glucagon should not be administered until the PET scanning has been completed.

Although it is desirable to complete MRI scanning within 45 min for the sake of patient comfort as well as economic considerations, this would be very challenging in colorectal imaging because of the need for high-resolution T2-weighted and diffusion-weighted images as well as contrast-enhanced T1-weighted images. In Fig. 4, we are proposing two PET/MRI workflows for colorectal imaging dedicated to sequential PET/MRI system. A PET/MRI scanning of the torso in one sweep, as it is being used for PET/CT, would not make sense for PET/MRI because of the complexity of the MRI pro-

cedure. Instead, the PET/MRI scanning is divided into two sections—head, neck, and chest; abdomen and pelvis. For head, neck, and chest areas, imaging may be limited to atMR for attenuation correction and mDIXON for anatomical localization with PET. For the abdomen and pelvis, a separate PET/MRI scanning with regional MRI sequences is justified to allow for a comprehensive MRI and PET correlation, Fig. 4. The separate PET/MRI scanning of head, neck, and chest from abdomen and pelvis will help improve imaging workflow and coregistration of PET and MRI data, particularly in the abdomen and pelvis because the two data sets are acquired immediately sequentially to each other. This also helps reduce unnecessary image acquisition and data

volume, allowing a faster data retrieval for image review. The bladder void between scan sections would help avoid misregistration of PET and MRI due to bladder filling, and improve lesion detection within the pelvis.

With the proposed workflow A in Fig. 4, it would be possible to reduce the acquisition time to 60 min. However, due to time constraints it will not be possible to use all the MRI sequences that are commonly used for the abdomen and pelvis in a stand-alone MRI system. The MRI protocol has to be trimmed to be able to achieve this 60-min benchmark (15 min pre- and post-contrast each). This workflow is however applicable for scanning with and without glucagon administration. Workflow B suits best for scanning without glucagon administration and has the advantage of shorter procedure time (90 vs. 130 min for workflow A) because the FDG uptake phase occurs while the patient is being scanned with MRI. In workflow A, the atMR sequence for attenuation correction of PET data is obtained before the administration of gadolinium agent, which was validated previously [26]. In workflow B, the atMR is acquired approximately 35 min after gadolinium administration, for which the effect of gadolinium on atMR attenuation map has not been validated. Acquiring the atMR sequence close to gadolinium administration will likely cause erroneous attenuation correction of PET, particularly in areas of large vessels and structures or lesions with contrast enhancement. However, this affect is least likely because 35 min has passed since the gadolinium administration, allowing a substantial amount of the contrast agent to be cleared from the blood pool and extracellular space [27]. In addition, the proposed bladder void before acquiring the atMR sequence will help reduce potential erroneous attenuation correction in the genitourinary system as well. Nevertheless, the effect of gadolinium on atMR attenuation correction is not clearly defined and should be validated in future studies.

As an alternative drug to glucagon, hyoscine *N*-butylbromide may be considered to relax the smooth muscles because it may not affect the PET images [25]. In this situation, MRI could be obtained first in parallel to the uptake phase and the PET scan would complete the PET/MRI examination. Hyoscine *N*-butylbromide is however not FDA approved and therefore cannot be used in the US although it has been widely utilized in Europe and Asia [28]. As MRI technology advances, novel MR sequences may be able to provide high quality MR images of the abdomen and pelvis in a considerably shorter time and help avoid bowel motion artifacts without the need for glucagon administration.

We acknowledge the small sample size of our report. Nevertheless, we think that our initial experience conveys valuable information in terms of diagnosis and workflow. Although clinical or imaging follow-up was used as part of reference standards, most key lesions in this report could be verified by histopathology. PET/CT was

acquired first in 9/12 patients, which represents an unfair advantage for PET/MRI in lesion detection because tumor uptake may increase over time. The glucose level was not measured prior to the FDG injection as per our clinical PET/CT protocol; thus, the effect of fasting glucose as well as the effect of glucagon on glucose level and muscular FDG uptake could not be further determined. The current study compares contrast-enhanced MRI with unenhanced, relatively low-dose CT (120 kVp with as low as 100 mAs), which may favor MRI in the localization of respective PET lesions.

## Conclusions

We have gained valuable information about the PET/MRI workflow using the Ingenuity TF PET/MRI for colorectal imaging, and our proposals regarding workflow provides the initial step in the evolving discussion of PET/MRI optimization for colorectal imaging. Because PET/CT was acquired first in most patients, there may be an unfair advantage for PET/MRI in lesion detection because tumor uptake increases over time. Our initial experience shows high diagnostic accuracy of PET/MRI in T staging of rectal cancer compared with PET/CT. In addition, PET/MRI shows at least comparable accuracy in N and M staging as well as restaging to PET/CT. However, the small sample size limits the generalizability of the results. PET/MRI may yield higher diagnostic accuracy than PET/CT considering the high soft tissue contrast provided by MRI compared with CT, but larger studies are necessary to fully assess the benefit of PET/MRI in colorectal cancer.

*Acknowledgement.* This study was sponsored by Philips Healthcare. We thank the staff at Philips Healthcare, Cleveland, Ohio, and especially Antonis Kalemis for his technical and scientific discussion.

## REFERENCES

- O'Neill BD, Brown G, Heald RJ, Cunningham D, Tait DM (2007) Non-operative treatment after neoadjuvant chemoradiotherapy for rectal cancer. *Lancet Oncol* 8(7):625–633. doi:10.1016/S1470-2045(07)70202-4
- Dewhurst CE, Mortele KJ (2013) Magnetic resonance imaging of rectal cancer. *Radiol Clin N Am* 51(1):121–131. doi:10.1016/j.rcl.2012.09.012
- Huebner RH, Park KC, Shepherd JE, et al. (2000) A meta-analysis of the literature for whole-body FDG PET detection of recurrent colorectal cancer. *J Nucl Med* 41(7):1177–1189
- Cohade C, Osman M, Leal J, Wahl RL (2003) Direct comparison of (18)F-FDG PET and PET/CT in patients with colorectal carcinoma. *J Nucl Med* 44(11):1797–1803
- Therasse P, Arbuck SG, Eisenhauer EA, et al. (2000) New guidelines to evaluate the response to treatment in solid tumors. European Organization for Research and Treatment of Cancer, National Cancer Institute of the United States, National Cancer Institute of Canada. *J Natl Cancer Inst* 92(3):205–216
- Monteil J, Mahmoudi N, Lebon S, et al. (2009) Chemotherapy response evaluation in metastatic colorectal cancer with FDG PET/CT and CT scans. *Anticancer Res* 29(7):2563–2568
- Kluza E, Rozeboom ED, Maas M, et al. (2013) T2 weighted signal intensity evolution may predict pathological complete response after treatment for rectal cancer. *Eur Radiol* 23(1):253–261. doi:10.1007/s00330-012-2578-z

8. Antoch G, Vogt FM, Freudenberg LS, et al. (2003) Whole-body dual-modality PET/CT and whole-body MRI for tumor staging in oncology. *JAMA* 290(24):3199–3206. doi:[10.1001/jama.290.24.3199](https://doi.org/10.1001/jama.290.24.3199)
9. Denecke T, Rau B, Hoffmann KT, et al. (2005) Comparison of CT, MRI and FDG-PET in response prediction of patients with locally advanced rectal cancer after multimodal preoperative therapy: is there a benefit in using functional imaging? *Eur Radiol* 15(8):1658–1666. doi:[10.1007/s00330-005-2658-4](https://doi.org/10.1007/s00330-005-2658-4)
10. Schmidt GP, Baur-Melynk A, Haug A, et al. (2009) Whole-body MRI at 1.5 T and 3 T compared with FDG-PET-CT for the detection of tumour recurrence in patients with colorectal cancer. *Eur Radiol* 19(6):1366–1378. doi:[10.1007/s00330-008-1289-y](https://doi.org/10.1007/s00330-008-1289-y)
11. Zaidi H, Ojha N, Morich M, et al. (2011) Design and performance evaluation of a whole-body Ingenuity TF PET-MRI system. *Phys Med Biol* 56(10):3091–3106. doi:[10.1088/0031-9155/56/10/013](https://doi.org/10.1088/0031-9155/56/10/013)
12. Kalemis A, Delattre BM, Heinzer S (2013) Sequential whole-body PET/MR scanner: concept, clinical use, and optimisation after two years in the clinic. The manufacturer's perspective. *Magma* 26(1):5–23. doi:[10.1007/s10334-012-0330-y](https://doi.org/10.1007/s10334-012-0330-y)
13. Kaur H, Choi H, You YN, et al. (2012) MR imaging for preoperative evaluation of primary rectal cancer: practical considerations. *Radiographics* 32(2):389–409. doi:[10.1148/Rg.322115122](https://doi.org/10.1148/Rg.322115122)
14. Drzezga A, Souvatzoglou M, Eiber M, et al. (2012) First clinical experience with integrated whole-body PET/MR: comparison to PET/CT in patients with oncologic diagnoses. *J Nucl Med* 53(6):845–855. doi:[10.2967/jnumed.111.098608](https://doi.org/10.2967/jnumed.111.098608)
15. Wiesmuller M, Quick HH, Navalpakkam B, et al. (2013) Comparison of lesion detection and quantitation of tracer uptake between PET from a simultaneously acquiring whole-body PET/MR hybrid scanner and PET from PET/CT. *Eur J Nucl Med Mol Imaging* 40(1):12–21. doi:[10.1007/s00259-012-2249-y](https://doi.org/10.1007/s00259-012-2249-y)
16. Gould MK, Maclean CC, Kuschner WG, Rydzak CE, Owens DK (2001) Accuracy of positron emission tomography for diagnosis of pulmonary nodules and mass lesions: a meta-analysis. *JAMA* 285(7):914–924
17. Donati OF, Hany TF, Reiner CS, et al. (2010) Value of retrospective fusion of PET and MR images in detection of hepatic metastases: comparison with 18F-FDG PET/CT and Gd-EOB-DTPA-enhanced MRI. *J Nucl Med* 51(5):692–699. doi:[10.2967/jnumed.109.068510](https://doi.org/10.2967/jnumed.109.068510)
18. Kohan AA, Kolthammer JA, Vercher-Conejero JL, et al. (2013) N staging of lung cancer patients with PET/MRI using a three-segment model attenuation correction algorithm: initial experience. *Eur Radiol* 23(11):3161–3169. doi:[10.1007/s00330-013-2914-y](https://doi.org/10.1007/s00330-013-2914-y)
19. Lee JW, Kim SK, Lee SM, Moon SH, Kim TS (2011) Detection of hepatic metastases using dual-time-point FDG PET/CT scans in patients with colorectal cancer. *Mol Imaging Biol* 13(3):565–572. doi:[10.1007/s11307-010-0394-x](https://doi.org/10.1007/s11307-010-0394-x)
20. Chong V (2004) The skull base in oncologic imaging. *Cancer Imaging* 4(1):5–6. doi:[10.1102/1470-7330.2003.0024](https://doi.org/10.1102/1470-7330.2003.0024)
21. Santini D, Tampellini M, Vincenzi B, et al. (2012) Natural history of bone metastasis in colorectal cancer: final results of a large Italian bone metastases study. *Ann Oncol* 23(8):2072–2077. doi:[10.1093/annonc/mdr572](https://doi.org/10.1093/annonc/mdr572)
22. Kershah S, Partovi S, Traughber BJ, et al. (2013) Comparison of standardized uptake values in normal structures between PET/CT and PET/MRI in an oncology patient population. *Mol Imaging Biol* 15(6):776–785. doi:[10.1007/s11307-013-0629-8](https://doi.org/10.1007/s11307-013-0629-8)
23. Kumar R, Loving VA, Chauhan A, et al. (2005) Potential of dual-time-point imaging to improve breast cancer diagnosis with (18)F-FDG PET. *J Nucl Med* 46(11):1819–1824
24. Chonde DB, Abolmaali N, Arabasz G, Guimaraes AR, Catana C (2013) Effect of MRI acoustic noise on cerebral fludeoxyglucose uptake in simultaneous MR-PET imaging. *Investig Radiol* 48(5):302–312. doi:[10.1097/RLI.0b013e3182839fbc](https://doi.org/10.1097/RLI.0b013e3182839fbc)
25. Yasuda S, Takechi M, Ono M, et al. (2012) The effect of glucagon on FDG uptake in skeletal muscle. *Tokai J Exp Clin Med* 37(1):11–13
26. Hu Z, Ojha N, Renisch S, Schulz V, Torres I, Buhl A, Pal D, Muswick G, Penatzer J, Guo T, et al. (2009) MR-based attenuation correction for a whole-body sequential PET/MR system. *IEEE Nucl Sci Conf Rec*:3508–3512
27. Aime S, Caravan P (2009) Biodistribution of gadolinium-based contrast agents, including gadolinium deposition. *J Magn Reson Imaging* 30(6):1259–1267. doi:[10.1002/jmri.21969](https://doi.org/10.1002/jmri.21969)
28. Froehlich JM, Daenzer M, von Weymarn C, et al. (2009) Aperistaltic effect of hyoscine *N*-butylbromide versus glucagon on the small bowel assessed by magnetic resonance imaging. *Eur Radiol* 19(6):1387–1393. doi:[10.1007/s00330-008-1293-2](https://doi.org/10.1007/s00330-008-1293-2)